in these organisms. Further experiments will be necessary to identify the pAL5 sequences responsible for CAT expression.

REFERENCES AND NOTES

1. D. A. Campbell, D. A. Thornton, J. C. Boothroyd, *Nature* **311**, 350 (1984); M. Milhausen, R. G. Nelson, S. Sather, M. Selkirk, N. Agabian, *Cell* **38**, 721 (1984); L. H. T. Van der Ploeg, A. W. C. A. Cornelissen, P. A. M. Michels, P. Borst, *ibid.* **39**, 213 (1984); J. C. Boothroyd, *Annu. Rev. Microbiol.* **39**, 475 (1985); P. Borst, *Annu. Rev. Biochem.* **55**, 701 (1986); L. H. T. Van der Ploeg, *Cell* **47**, 479 (1986); W. J. Murphy, K. P. Watkins, N. Agabian, *ibid.*, p. 517; R. E. Sutton and J. C. Boothroyd, *ibid.*, p. 527; C. E. Clayton, *Genetic Eng.* 7, 1 (1988).
2. J. M. Kooter, T. De Lange, P. Borst, *EMBO J.* **3**, 2387 (1984); J. M. Kooter and P. Borst, *Nucleic Acids Res.* **12**, 9457 (1984).
3. M. L. Muhich and J. C. Boothroyd, *Mol. Cell. Biol.* **8**, 3837 (1988).
4. V. Bellofatto and G. A. M. Cross, *Nucleic Acids Res.* **16**, 3455 (1988).
5. A. Gonzalez *et al.*, *ibid.* **13**, 5789 (1985); M. A. Imboden, P. W. Laird, M. Affolter, T. Seebeck, *ibid.* **15**, 7357 (1987); P. J. Johnson, J. M. Kooter, P. Borst, *Cell* **51**, 273 (1987). W. C. Gibson, B. W. Swinkels, P. Borst, *J. Mol. Biol.* **201**, 315 (1988); C. Tschudi and E. Ullu, *EMBO J.* 7, 455 (1988).
6. V. Bellofatto, R. Cooper, G. A. M. Cross, *Nucleic Acids Res.* **16**, 7437 (1988).
7. S. I. Miller, S. M. Landfear, D. F. Wirth, *ibid.* **14**, 7341 (1986); M. Parsons, R. G. Nelson, N. Agabian, *ibid.*, p. 1703; G. A. Cook and J. E. Donelson, *Mol. Biochem. Parasitol.* **25**, 113 (1987); M. L. Muhich, D. E. Hughes, A. M. Simpson, L. Simpson, *Nucleic Acids Res.* **15**, 3141 (1987).
8. T. De Lange *et al.*, *Nucleic Acids Res.* **12**, 4431 (1984); A. Gabriel, S. S. Sisodia, D. W. Cleveland, *J. Biol. Chem.* **262**, 16192 (1987).
9. K. L. Perry, K. P. Watkins, N. Agabian, *Proc. Natl. Acad. Sci. U.S.A.* **84**, 8190 (1987); M. S. Freistadt, G. A. M. Cross, A. D. Branch, H. Robertson, *Nucleic Acids Res.* **15**, 9861 (1987).
10. W. C. Gibson, T. C. White, P. W. Laird, P. Borst, *EMBO J.* **6**, 2457 (1987); J. Eid and B. Sollner-Webb, *Proc. Natl. Acad. Sci. U.S.A.* **84**, 7812 (1987). In a letter circulated to colleagues in the field, Drs. Eid and Sollner-Webb have drawn attention to problems of interpretation of their published data.
11. D. E. Hughes and L. Simpson, *Proc. Natl. Acad. Sci. U.S.A.* **83**, 6058 (1986).
12. J. A. Walder *et al.*, *Science* **233**, 569 (1986); A. W. C. A. Cornelissen *et al.*, *Nucleic Acids Res.* **14**, 5605 (1986).
13. U. Zimmerman, P. Scheurich, G. Pilwat, R. Benz, *Angewandte Chemie* **20**, 325 (1981).
14. C. Gorman *et al.*, *Mol. Cell. Biol.* **2**, 1044 (1982).
15. V. Bellofatto, unpublished data.
16. C. A. Bunker and D. D. Moore, *Gene* **67**, 279 (1988).
17. R. Brun and M. Schonenberger, *Z. Parasitenkd.* **66**, 17 (1979).
18. V. Bellofatto, A. H. Fairlamb, G. B. Henderson, G. A. M. Cross, *Mol. Biochem. Parasitol.* **25**, 227 (1987).
19. B. Seed and J. Sheen, *Gene* **67**, 271 (1988).
20. The authors thank C. G. Clark, P. Model, and D. Sherman for useful discussions, C. E. Clayton for critical reading of the manuscript, and A. Molloy for assistance in the construction of pAL1. pSV2CAT was a generous gift from B. H. Howard. Supported by NIH grant AI21729.

17 January 1989; accepted 18 April 1989

Rhenium-Osmium and Samarium-Neodymium Isotopic Systematics of the Stillwater Complex

DAVID D. LAMBERT,* JOHN W. MORGAN, RICHARD J. WALKER, STEVEN B. SHIREY, RICHARD W. CARLSON, MICHAEL L. ZIENTEK, MICHAEL S. KOSKI

Isotopic data for the Stillwater Complex, Montana, which formed about 2700 Ma (million years ago), were obtained to evaluate the role of magma mixing in the formation of strategic platinum-group element (PGE) ore deposits. Neodymium and osmium isotopic data indicate that the intrusion formed from at least two geochemically distinct magmas. Ultramafic affinity (U-type) magmas had initial ε_{Nd} of -0.8 to -3.2 and a chondritic initial $^{187}\text{Os}/^{186}\text{Os}$ ratio of ~ 0.88, whereas anorthositic affinity (A-type) magmas had ε_{Nd} of -0.7 to $+1.7$ and an initial $^{187}\text{Os}/^{186}\text{Os}$ ratio of ~ 1.13. These data suggest that U-type magmas were derived from a lithospheric mantle source containing recycled crustal materials whereas A-type magmas originated either by crustal contamination of basaltic magmas or by partial melting of basalt in the lower crust. The Nd and Os isotopic data also suggest that Os, and probably the other PGEs in ore horizons such as the J-M Reef, was derived from A-type magmas. The Nd and Os isotopic heterogeneity observed in rocks below the J-M Reef also suggests that A-type magmas were injected into the Stillwater U-type magma chamber at several stages during the development of the Ultramafic series.

MAFIC LAYERED INTRUSIONS ARE the world's major repositories of nickel, chromium, and PGEs. Much of the petrologic and geochemical information concerning the evolution of mantle-derived magmas in large crustal-level magma chambers is in part a result of the intensive study of these mineral deposits in intrusions such as the Bushveld Complex of South Africa and the Great Dyke of Zimbabwe. The Stillwater Complex is an Archean mafic layered intrusion exposed in a belt approximately 45 km long and 6 km wide in the Beartooth Mountains, Montana. Magmas parental to the complex intruded metamorphic rocks of the Wyoming craton having ages of 3200 to 2750 Ma (*1*). The age of the Stillwater Complex is constrained to 2701 ± 41 Ma by several isotopic techniques [reviewed in (*2*)]. Five major stratigraphic subdivisions of the complex have been recognized (*3*): the Basal series (BS), the Ultramafic series (UMS), and the Lower, Middle, and Upper Banded series (LBS, MBS, and UBS, respectively) (Fig. 1). Magnesium-rich olivine appears as a cumulus phase only in five zones throughout the LBS, MBS, and UBS. These have been referred to as Olivine-bearing zones [OBZs (*3, 4*)] or Troctolite-Anorthosite zones (*3, 5*). The PGE-rich horizon of the Stillwater Complex, informally named the J-M Reef (*5*), occurs as a relatively thin (1 to 3 m) layer along nearly the entire 45-km length of the intrusion, approximately 400 m above the top of the UMS in OBZ I (Fig. 1).

Recent models for the formation of PGE deposits in mafic layered intrusions have emphasized the role of magma mixing (*5–8*). In the Stillwater Complex, two geochemically distinct magma types have been proposed: U-type magmas that were enriched in MgO and SiO_2 [similar to modern olivine boninites (*9, 10*)], and A-type magmas that were enriched in Al_2O_3 [similar to modern high-Al tholeiitic basalts (*9*)]. Phase equilibria studies have demonstrated that both A-type magmas and mixtures of U- and A-type magmas have a paragenetic sequence appropriate for OBZ I and the J-M Reef, which is olivine followed by plagioclase (*6, 9*). This sequence is different from that in the UMS, which is olivine followed by orthopyroxene (*5*). Mixing of compositionally disparate magmas may also have had a profound influence on the degree of sulfur saturation (*6, 7*). Because sulfide melt–silicate melt partition coefficients for the PGEs are large [$>10^5$ for the J-M Reef (*7*)], an immiscible sulfide melt that formed as a result of magma mixing would act as a collector of the PGEs (*7*). Hence, mixing of magmas with contrasting major and trace

---

D. D. Lambert, S. B. Shirey, R. W. Carlson, Department of Terrestrial Magnetism, Carnegie Institution of Washington, 5241 Broad Branch Road, NW, Washington, DC 20015.
J. W. Morgan and R. J. Walker, U.S. Geological Survey, Mail Stop 981, Reston, VA 22092.
M. L. Zientek, U. S. Geological Survey, 345 Middlefield Road, Mail Stop 901, Menlo Park, CA 94025.
M. S. Koski, Stillwater Mining Company, Star Route 2, Box 365, Nye, MT 59061.

*To whom correspondence should be addressed.

element composition, PGE abundances, and sulfur solubilities may have been fundamental to the formation of the PGE ore deposit (*5, 6*). If such mixing occurred, the compositional and isotopic characteristics of olivine- and sulfide-bearing stratigraphic intervals such as OBZ I should reflect mixing between the two magma types (*8*).

Earlier workers have proposed that the PGEs (especially the more incompatible Pt and Pd) in the J-M Reef were derived from U-type magmas (*5, 6, 8, 11*). Sulfur, necessary for the formation of the PGE-rich sulfide minerals observed in the J-M Reef (*5*), was thought to be derived from a major injection of new magma into the chamber (*5, 7, 8*). We have obtained Rb-Sr and Sm-Nd isotopic data for 20 cumulate rocks, three fine-grained sills or dikes, and one footwall hornfels. Re-Os isotopic data have been obtained for cumulates from the J-M Reef and other sulfide- and chromite-bearing horizons of the intrusion. In concert, these isotopic systems allow us to evaluate the role of magma mixing in the formation of the PGE ore deposit and to characterize the magma sources. The Re-Os isotopic system may be particularly useful in investigating the sources of precious metals in ore deposits because Os is one of the six PGE.

Earlier Rb-Sr isotopic data for rocks and minerals from the Stillwater Complex (*12, 13*) and our whole rock Rb-Sr isotopic data (not shown, available on request) define a scattered array with an age of approximately 1100 Ma, much younger than the crystallization age of 2700 Ma. These data demonstrate that the Rb-Sr isotopic system in these rocks has not remained closed, but was disturbed as a result of one or more thermal metamorphic events during the Proterozoic.

Earlier Sm-Nd isotopic data for minerals from an LBS gabbronorite (*13*) define an isochron with an age of 2701 ± 41 Ma and an initial Nd isotopic composition of $\varepsilon_{Nd} = -2.0 \pm 1.2$ (Table 1), for the isochron regression treatment of (*14*). Apparent Nd isotopic homogeneity of the intrusion was implied by whole rock Nd isotopic data for only five cumulates (orthopyroxenite, norite, anorthosite, and gabbros) (*13*). We have now analyzed many samples that extend over a much greater stratigraphic interval. Most of our data for anorthosites and troctolites from the Anorthosite and Olivine-bearing zones (Table 1 and Figs. 1 and 2), plot well above this 2701 Ma mineral isochron. In addition, two Cu-Ni sulfide-rich ultramafic cumulates from the UMS collected near the base of the complex (355-64-463.8, and 355-64-556.0) and a chromitite collected near an alaskite sill in the MBS (88PPT10) have initial ε_{Nd} values below the isochron ($\varepsilon_{Nd} = -3.5$ to -5.6; Table 1 and Fig. 2).

The low ε_{Nd} values of these three samples may reflect derivation from magmas locally contaminated with Archean upper crustal rocks, which had ε_{Nd} values at 2701 Ma of -3 to -6 (355-64-927.5 of Table 1 and Fig. 2). Alternatively, these low ε_{Nd} values may reflect the effects of postmagmatic hydrothermal alteration. These samples show petrographic evidence for the introduction of fluids potentially derived from the adjacent country rocks. For example, abundant quartz is observed in chromitite sample 88PPT10. Local contamination near the base of the intrusion also has affected Pb (*15*) and S (*16*) isotopes in the BS and lower UMS. However, chromitite 79LM39 collected near the top of the UMS has a high initial ε_{Nd} value (+1.2; Table 1 and Fig. 2), which suggests that in situ contamination occurred only near the base of the intrusion.

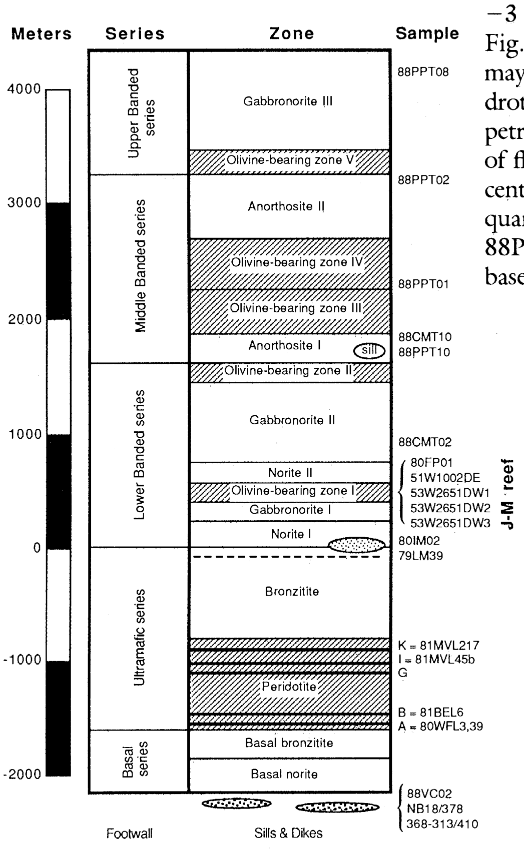

Fig. 1. Stratigraphic subdivisions of the Stillwater Complex, after (*3*). Stratigraphic height is measured relative to the Ultramafic series–Lower Banded series contact. Olivine-bearing portions of the complex are denoted with a ruled pattern. Solid or dashed horizontal lines in the Peridotite and Bronzitite zones denote chromitite layers analyzed in this study. Approximate sample locations and numbers are shown to the right of the stratigraphy. "Dotted pod" at the top of the Ultramafic series denotes the location of a bronzite pegmatite (80IM02). "Sill" in Anorthosite zone I shows the location of an intrusive alaskite sill with selvages of chromite- and sulfide-rich rock (88PPT10). The locations of five sulfide-bearing rocks from the J-M Reef are shown in Olivine-bearing zone I. Six closely spaced samples from AMAX drill core 355-64 that brackets the Basal series-Ultramafic series contact are not shown.

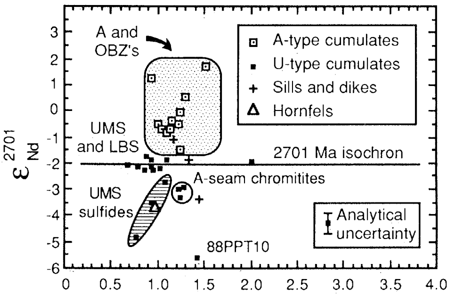

Fig. 2. Initial Nd isotopic composition (ε_{Nd} at 2701 Ma) versus chondrite-normalized Nd/Sm diagram for whole rocks and minerals from the Stillwater Complex [includes data from (*13*)]. Samples have been subdivided on the basis of magmatic affinities [U-type cumulates and A-type cumulates (*6*)]. Abbreviations: UMS, Ultramafic series samples; LBS, Lower Banded series samples; A and OBZ's, Anorthosite and Olivine-bearing zone samples. The three chromitite analyses are from the UMS; 2701-Ma mineral isochron (*13*) and typical analytical uncertainty in ε_{Nd} (95% confidence level) are shown for reference.

Barring post-crystallization disturbance, which is not likely for the Sm-Nd system, the Nd isotopic systematics of these rocks from the Stillwater Complex preclude the interpretation that the intrusion formed from one isotopically homogeneous magma. When the samples from this and the earlier study (*13*) are grouped according to U- and A-type magmatic affinities (*6*), unaltered cumulates that are thought to have crystallized from U-type magmas have initial ε_{Nd} of -0.9 to -3.0, consistent with the initial isotopic composition of the Sm-Nd mineral isochron [(*13*), Fig. 2]. This low ε_{Nd} value suggests that a component of the U-type magma had a long-term history of light rare earth element (REE) enrichment. In contrast, cumulates that crystallized from A-type magmas, in particular samples from Olivine-bearing zones and Anorthosite zones of the LBS and MBS (Figs. 1 and 2) plot above the mineral isochron with initial ε_{Nd} of -0.8 to $+1.7$ (Fig. 2). The high ε_{Nd} values of these cumulates suggest that they crystallized from A-type magmas derived from an isotopically different source that had a long-term history of chondritic to slightly depleted light REE abundances.

The high initial ε_{Nd} (+1.2) for chromitite sample 79LM39 from the top of the UMS (Fig. 1) suggests that some A-type magma was injected into the U-type magma at this level in the intrusion, consistent with REE data across this same interval (*17*). The major change in ε_{Nd} from U-type to A-type magmatic affinity occurs over the ~1-m sample interval at the base of OBZ I, just below the J-M Reef (*18*). A gabbronorite with U-type magmatic affinity immediately below OBZ I has an ε_{Nd} of −1.9 (sample 53W2651DW3). Troctolites and anorthosites of the main ore zone in OBZ I (samples 53W2651DW 2 and 1, respectively) have an ε_{Nd} of −0.5 to −0.4. One analysis of a massive sulfide pod from the main ore zone (51W1002DE) has an ε_{Nd} of +1.7, the highest initial Nd isotopic compositon that was measured (Fig. 2). Field observations of highly disturbed slump layering and ultramafic xenoliths near the base of OBZ I (*5*) are indicative of a disturbance in the magma chamber and suggest that regular crystallization of the UMS and LBS may have been interrupted by the introduction of new magma. The abrupt changes in paragenetic sequence (*5, 6*), REE ratios (*8*), and initial ε_{Nd} across this stratigraphic boundary are consistent with this interpretation.

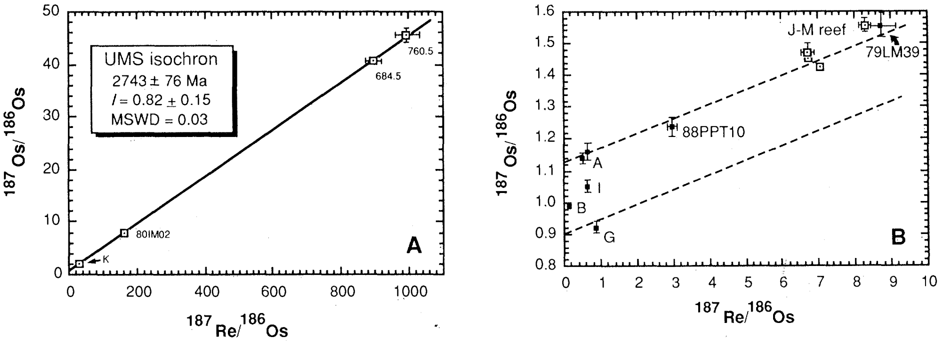

Fig. 3. (**A**) $^{187}Re/^{186}Os$ versus $^{187}Os/^{186}Os$ isochron diagram for four samples from the Ultramafic series (UMS) of the Stillwater Complex with $^{187}Re/^{186}Os$ ratios >28 (Table 2); I, initial $^{187}Os/^{186}Os$ ratio; MSWD, mean square of weighted deviates. (**B**) Detail of Re-Os isochron diagram for 11 samples from the Stillwater Complex with $^{187}Re/^{186}Os$ ratios <10; open boxes are sulfide-bearing samples from the J-M Reef and filled boxes are chromitites; a 2701-Ma chondritic reference isochron is shown as a dashed line with an initial Os isotopic composition of 0.90. The upper dashed line represents a 2701-Ma reference isochron through eight analyses with an initial Os isotopic composition of 1.13. Errors at the 95% confidence level are shown with bars or are entirely within the symbol.

Sills and dikes associated with the Stillwater Complex are thought to represent the original magmas that produced the cumulate rocks of the intrusion (*19*). We have analyzed three of the five petrologic varieties of sills and dikes that have been recognized (*19*) (Fig. 2). A gabbronorite sill (group 1, 368-313/410) plots within the field of A-type cumulates, consistent with REE data which suggest that this sill type may represent A-type magmas (*8*). However, these sills may not have major element characteristics appropriate for the proposed A-type magmas (*19*). A high-MgO gabbronorite sill (group 2, NB 18/378) plots within analytical uncertainty of the 2701 Ma mineral isochron, also consistent with REE (*8*) and major element data (*19*) that suggest this sill type may represent U-type magmas or their derivatives. Mafic norite sills also have been considered to represent U-type magma (*19*). One analysis of this type of sill (group 3, 88VC02) plots near analyses of sulfide- and chromite-rich cumulates from the UMS, consistent with this interpretation.

Table 1. Abundances of Sm and Nd and Nd isotopic composition for cumulate whole rocks from the Stillwater Complex, Montana; Nd isotope analyses (*34*) are fractionation-corrected to $^{146}Nd/^{144}Nd$ = 0.72190 and reported relative to $^{143}Nd/^{144}Nd$ on the La Jolla Nd standard of 0.511860. Uncertainties for Nd isotopic composition (in last significant figures in parentheses) are 2σ of the population (0.000020) for repeat standard analyses (n = 30) or represent internal precision of 200 to 300 ratios (if >0.000020) and correspond to last digit. Total analytical blanks for Sm and Nd measured for the procedures used in this study that were designed for large (0.5 g) samples are less than 17 and 75 pg, respectively; ε_{Nd} (2701 Ma) is defined as the deviation at the crystallization age in parts per 10,000 from the isotopic composition in a chondritic reference reservoir with a present-day $^{143}Nd/^{144}Nd$ ratio = 0.512636 and a $^{147}Sm/^{144}Nd$ ratio = 0.1967.

Sample	Location*	Sm (ppm)	Nd (ppm)	$^{147}Sm/^{144}Nd$	$^{143}Nd/^{144}Nd$	ε_{Nd} (2701 Ma)
88PPT08	UBS-GN III	0.655	2.15	0.1844	0.512381(20)	−0.71
88PPT02	MBS-AN II	0.466	1.65	0.1705	0.512131(20)	−0.73
88PPT01	MBS-OBZ IV	0.312	1.25	0.1505	0.511840(20)	0.55
88CMT10	MBS-AN I	0.257	0.884	0.1756	0.512216(20)	−0.85
88PPT10	MBS-AN I(chromitite)	0.253	1.12	0.1365	0.511279(28)	−5.6
88CMT02	LBS-GN II	0.600	1.89	0.1920	0.512527(20)	−0.51
80FP01	LBS-OBZ I (J-M Reef)	0.097	0.386	0.1524	0.511845(20)	−0.04
51W1002DE	LBS-OBZ I (J-M Reef)	0.006	0.027	0.1283	0.511503(25)	1.7
53W2651DW1	LBS-OBZ I (J-M Reef)	0.170	0.611	0.1684	0.512112(20)	−0.38
53W2651DW2	LBS-OBZ I (J-M Reef)	0.156	0.591	0.1592	0.511943(30)	−0.49
53W2651DW3	LBS-GN I (J-M Reef)	0.208	0.722	0.1743	0.512141(22)	−1.9
80IM02	UMS-BZ (pegmatite)	0.362	0.988	0.2215	0.512991(20)	−1.7
79LM39	UMS-BZ (chromitite)	0.108	0.316	0.2075	0.512891(28)	1.2
80WFL3	UMS-PZ (A chromitite)	0.084	0.331	0.1532	0.511714(59)	−2.9
80WFL39	UMS-PZ (A chromitite)	0.045	0.174	0.1554	0.511733(24)	−3.3
355-64-160.5	UMS-PZ (chromitite)	0.078	0.294	0.1593	0.511816(21)	−3.0
355-64-463.8	UMS-PZ (sulfides)	0.180	0.518	0.2094	0.512682(21)	−3.5
355-64-556.0	UMS-PZ (sulfides)	0.077	0.181	0.2557	0.513422(22)	−5.2
355-64-684.5	UMS-PZ (sulfides)	0.029	0.101	0.1752	0.512114(20)	−2.7
355-64-927.5	Footwall (hornfels)	0.176	0.528	0.2014	0.512534(20)	−3.7
88VC02	Footwall (Group 3 sill)	1.41	6.37	0.1339	0.511346(20)	−3.4
NB18/1378	Footwall (Group 2 sill)	3.53	14.6	0.1466	0.511647(20)	−1.9
368-313/410	Footwall (Group 1 sill)	3.79	13.8	0.1659	0.512031(20)	−1.1

*Series or zone for nomenclature of (*3*).

The Re-Os isotopic data for 15 whole rocks (Table 2) exhibit a large spread in $^{187}Re/^{186}Os$ ratios (0.150 to 997). Two sulfide-rich cumulates from the BS and UMS (355-64-684.5 and 355-64-760.5), the K-seam chromitite (81MVL217), and a bronzite pegmatite from the top of the UMS (80IM02) that have $^{187}Re/^{186}Os$ ratios >28 define an isochron with an age of 2743 ± 76 Ma and an initial Os isotopic composition of 0.82 ± 0.15 (Fig. 3A). This age was calculated with a ^{187}Re decay constant of 1.59×10^{-11} $years^{-1}$ (*20*). Because these four samples have high $^{187}Re/^{186}Os$ ratios, the age is relatively insensitive to variations in the initial isotopic composition of the parental magmas (described below). The low MSWD (Fig. 3A) suggests that the scatter about the line can be accounted for by analytical error. This age is within analytical uncertainty of the Sm-Nd mineral isochron age of 2701 ± 41 Ma for the LBS gabbronorite (*13*), and overlaps a U-Pb age of 2667 ± 3 Ma for zircons from OBZ I (*2*) and a Pb-Pb isochron age of 2662 ± 24 Ma for six whole rocks (*21*). Currently available isotopic data for the footwall sills and dikes that may be contemporaneous with emplacement of the Stillwater Complex (*22*) are also consistent with this Re-Os isochron age. The linearity of the Re-Os data demonstrates that the Re-Os isotopic systematics in these parts of the Stillwater Complex have not been disturbed by later events, unlike the Rb-Sr isotopic systematics [see also (*13*)]. This large, apparently magmatic range in Re/Os ratios indicates that this system has broad applications in the geochronology of mafic-ultramafic rocks and magmatic ore deposits.

Significant initial Os isotopic heterogeneities are revealed for samples with ^{187}Re/^{186}Os ratios <10 (Fig. 3B). The results suggest that the unmodified U-type magma had a nearly chondritic initial ^{187}Os/^{186}Os ratio and that the A-type magma, in contrast, was considerably enriched in ^{187}Os. For example, Re-Os isotopic data for the G-seam chromitite (Fig. 3B) plot within uncertainty of a 2701 Ma reference isochron with a chondritic initial ^{187}Os/^{186}Os of 0.90 (*23*). This suggests that at least some parts of the UMS crystallized from magmas with an Os isotopic composition no more radiogenic than chondritic mantle (Fig. 3B); this composition is comparable to the source composition identified for a suite of $\sim$2700 Ma komatiites from the Superior Province, Canada (*24*). In contrast to the data for the G-seam chromitite, data for the A-seam, B-seam, and I-seam chromitites from the lower UMS, a thin chromitite near the UMS-LBS contact, four sulfide-bearing samples from the PGE-rich J-M Reef, and a PGE-enriched chromitite near the alaskite sill in the MBS plot above the chondritic reference isochron (Fig. 3B). These ten samples have calculated initial ^{187}Os/^{186}Os ratios at 2701 Ma of 0.98 to 1.18, compositions that are 8 to 31% enriched in ^{187}Os relative to the chondritic initial Os isotopic composition (Fig. 3B). These data imply that Os was derived from at least two isotopically distinct magmas that were injected periodically into the Stillwater magma chamber, consistent with the heterogeneities observed in the Nd isotopic data (Fig. 2). The Os isotopic contrast between the PGE-enriched A-seam chromitite from the base of the complex and the G-seam chromitite from higher in the UMS (Fig. 3B) corroborates the suggestion (*9*) that the introduction of geochemically distinct magmas early in the development of the magma chamber may have played an important role in the formation of some chromitite layers. Although the Os isotopic variations do not directly correspond with the Nd isotopic variations in the chromitites, the Nd isotopic evidence for the effect of A-type magma on the crystallization of the A-seam chromitite may have been obscured by in situ contamination of these ultramafic rocks near the base of the intrusion.

The enriched Os isotopic composition of the J-M Reef appears to be typical of magmas that have A-type affinities as based on their Nd isotopic compositions and mineral paragenesis (*5*, *6*). The relatively uniform enrichment in ^{187}Os in samples from the J-M Reef may indicate that the initial Os isotopic composition of the A-type magma was approximately 1.13 (Fig. 3B). Hence, the Os isotopic data are consistent with derivation of the Os (and therefore probably the other PGEs) in the J-M Reef from the A-type magma rather than from the U-type magma, in contrast to the interpretations of earlier workers. This enriched initial Os isotopic composition also occurs in other samples that contain anomalously high concentrations of PGEs, such as the A- and B-seam chromitites, compared to other cumulates of the UMS (*25*, *26*). Thus, the high initial Os isotopic composition of other PGE-enriched sulfide and chromitite horizons may be the result of extraction of the PGEs from injections of A-type magma into the chamber below the stratigraphic level of the J-M Reef, but not in significant amounts that would tend to dominate the Nd isotopic composition of the UMS. Phase equilibria studies suggest that each pulse of A-type magma may yield chromite or an immiscible sulfide melt upon mixing with U-type magmas (*9*). By analogy, PGE ore horizons in other mafic-layered intrusions may have formed as a result of magma mixing and extraction of the noble metals from large volumes of basaltic magma with the aid of an immiscible sulfide melt.

Table 2. Re and Os abundances and Os isotopic compositions in cumulate whole rocks from the Stillwater Complex, Montana; Os concentrations are reported as common Os calculated for a ^{187}Os/^{186}Os ratio at 2701 Ma of 0.90; procedures are described in (*23*) and (*34*). Uncertainties for the Re-Os isotopic data (in last significant figures in parentheses) are predominantly controlled by counting statistics as described in (*34*). Total analytical blanks for Re and Os are less than 60 pg and 2 pg, respectively.

Sample	Re (ppb)	Os (ppb)	^{187}Re/^{186}Os	^{187}Os/^{186}Os	^{187}Os/^{186}Os (2701 Ma)
88PPT10	7.98(24)	108(2)	2.97(12)	1.24(3)	1.11
51W1002DE	754(7)	4270(46)	7.09(10)	1.42(01)	1.11
53W2651DW1	9.23(14)	54.7(8)	6.78(17)	1.47(3)	1.17
(duplicate)		[48.5(2.2)]		[1.42(2)]	
53W2651DW2	11.06(14)	53.6(69)	8.27(16)	1.55(2)	1.18
53W2651DW3	21.5(2)	139(1)	6.20(11)	1.42(1)	1.15
80IM02	24.4(6)	6.10(12)	160(4.8)	7.98(32)	0.96
79LM39	1.46(6)	6.77(10)	8.73(40)	1.55(4)	1.17
81MVL217 (K chromitite)	0.675(21)	0.943(19)	28.7(1.3)	2.10(11)	0.84
81MVL45b (I chromitite)	0.536(27)	33.7(1.35)	0.638(41)	1.05(2)	1.02
G chromitite	0.993(50)	46.7(8)	0.852(47)	0.918(17)	0.88
81BEL6 (B chromitite)	0.408(20)	109(1)	0.150(8)	0.989(10)	0.98
80WFL3	1.11(2)	67.3(9)	0.660(20)	1.16(3)	1.13
80WFL39	1.69(3)	133(2)	0.511(13)	1.14(2)	1.12
(duplicate)	[1.65(5)]	[107(2)]	[0.617(25)]	[1.14(2)]	(111)
355-64-6845	87.8(18)	3.87(4)	892(22)	40.5(8)	1.36
355-64-7605	30.7(5)	1.23(5)	997(40)	45.5(1.1)	1.75
88VC02		0.821(31)			

The origin of this isotopically enriched A-type magma probably is not consistent with the involvement of a subcontinental mantle source enriched in the large ion lithophile elements (LILE), as has been proposed (*27*, *28*). The one example of LILE-enriched lithosphere studied thus far with the Re-Os isotopic system displays chondritic to substantially less than chondritic ^{187}Os/^{186}Os ratios (*29*). The Nd and Os isotopic systematics also clearly preclude the interpretation that A-type magma was derived from a mantle source that had obtained an enriched isotopic signature as a result of the addition of crustal components in the mantle (*30*). Recycling of oceanic or continental crust into the mantle via subduction has a minimal effect on the Os isotopic composition of the mantle (Fig. 4) because of the high Os concentration in the mantle and the only 5- to 10-fold enrichment of Re in the crust relative to the mantle (*31*). The Os isotopic composition of the mantle essentially is buffered near chondritic values [0.90 at 2701 Ma (*23*)] for even large amounts ($>50\%$) of addition of crustal materials (Fig. 4), unlike the Rb-Sr and Sm-Nd systems (*29*).

Because of the low Os concentration in basaltic magmas (*32*), A-type magmas could have become enriched in radiogenic Os if contaminated with the surrounding older Archean crustal rocks of the Beartooth Mountains (*1*, *27*). For example, addition of $<10\%$ model Archean crust ($\varepsilon_{Nd} = -5$; ^{187}Os/^{186}Os ratio = 5; 0.05 ppb Os) to a mantle-derived basalt at 2701 Ma would

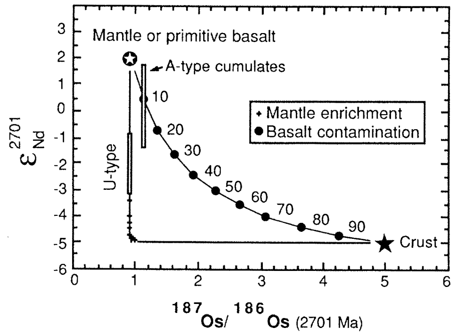

Fig. 4. Initial Nd isotopic composition (ε_{Nd} at 2701 Ma) versus initial $^{187}Os/^{186}Os$ diagram illustrating the effects of crustal contamination on the isotopic composition of mantle-derived tholeiitic basalt and the enrichment of the mantle with older crustal components. The star-labeled "Crust" represents the calculated isotopic composition of hypothetical Archean continental crust of the Wyoming craton with 20 ppm Nd (*35*) and 0.05 ppb Os (*31*), a $^{187}Re/^{186}Os$ ratio of 500 (*32*), and a crustal residence time of 500 million years [based on a model mantle separation ages of 3200 Ma (*1, 26*)]. The "Mantle" star has the Nd isotopic composition of average depleted mantle at 2701 Ma [ε_{Nd} = +2 (*36*)] and lies on the chondritic Os isotopic growth curve at 2701 Ma [0.90 (*23*)] and has assumed concentrations of 1.5 ppm Nd and 4 ppb Os (*31*). "Primitive Basalt" has the same isotopic composition as "Mantle" but with assumed concentrations of 8 ppm Nd and 0.1 ppb Os (*32*). The curves connecting these points (mantle-crust or primitive basalt–crust) show the isotopic composition of mixtures of the two end members with tick marks or circles on the curves marking 10% increments of crustal mixing (labeled on one curve for reference). Neodymium and osmium isotopic compositional ranges of unmodified Stillwater U-type and A-type cumulates are shown as boxes.

result in a Nd and Os isotopic composition similar to the proposed A-type magmas parental to the J-M Reef (Fig. 4). The uniformly high initial $^{187}Os/^{186}Os$ ratios (1.11 to 1.18) for many cumulates with A-type magmatic affinity from widely spaced locations in the intrusion, however, suggest that contamination would have to have occurred before emplacement and not as a result of in situ contamination.

Alternatively, partial melting of juvenile basaltic rocks in the lower crust (15- to 20-kbar pressure), leaving a pyroxene-dominated residue (*33*), could account for the Nd and Os isotopic data. For example, basaltic rocks with a $^{187}Re/^{186}Os$ ratio = 1500 (*32*) will evolve to the high initial Os isotopic composition of the A-type magmas within 10 Ma following their extraction from the mantle. This short crustal residence time also would preserve the relatively high $^{143}Nd/^{144}Nd$ ratios ($\varepsilon_{Nd} \geq 0$) in A-type cumulates that was inherited from the magmatic source.

The Nd and Os isotopic requirements for the source of the Stillwater U-type magma are distinctly different. Data for rocks of the UMS suggest that unmodified U-type magmas had chondritic Os isotopic compositions (based on the G-seam chromitite data) but significantly lower than chondritic Nd isotopic compositions (ε_{Nd} = −0.8 to −3.2). The Nd isotopic characteristics are consistent with derivation of U-type magmas by ~35% contamination of mantle-derived basaltic komatiite with older Archean crust before intrusion. If the U-type magma had >1 ppb Os, considerable crustal contamination would have produced a minimal effect on the Os isotopic composition of the magma, as is observed in Stillwater U-type cumulate rocks analyzed in this study. However, if the U-type magmas had Os concentrations comparable to or lower than the group 3 mafic norite (0.821 ppb; sample 88VC02, Table 2), such a large amount of contamination would elevate the initial $^{187}Os/^{186}Os$ ratio significantly above chondritic (if the Archean crustal contaminant had 0.05 ppb Os and a $^{187}Os/^{186}Os$ ratio of 5). Alternatively, the Nd and Os isotopic requirements are also consistent with enrichment of the mantle source of U-type magmas by ~9% recycled Early to Middle Archean continental crust of the Wyoming craton that is ~500 million years older than the Stillwater Complex (*1, 27*). This enrichment process would strongly affect the Nd isotopic composition of the source region but not the Os isotopic composition because of the high Os concentration in the mantle before enrichment (Fig. 4). Partial melting (~20%) of this enriched subcontinental mantle source would yield magmas with isotopic and trace element characteristics similar to Stillwater U-type magmas.

REFERENCES AND NOTES

1. D. J. Henry *et al.*, in *Precambrian Geology of the Beartooth Mountains, Montana and Wyoming*, P. A. Mueller and J. L. Wooden, Eds. (*Spec. Publ. 84*, Montana Bureau Mines and Geology, Butte, 1982), pp. 147–156; P. A. Mueller *et al.*, in *Stillwater Complex*, G. K. Czamanske and M. L. Zientek, Eds. (*Spec. Publ. 92*, Montana Bureau of Mines and Geology, Butte, 1985), pp. 9–20; J. L. Wooden and P. M. Mueller, *Geol. Soc. Am. Abst. Prog.* **19**, 896 (1987).
2. D. D. Lambert *et al.*, in *Stillwater Complex*, G. K. Czamanske and M. L. Zientek, Eds. (*Spec. Publ. 92*, Montana Bureau of Mines and Geology, Butte, 1985), pp. 46–54.
3. M. L. Zientek *et al.*, in *ibid.*, pp. 21–32.
4. I. S. McCallum *et al.*, *Am. J. Sci.* **280A**, 59 (1980).
5. S. G. Todd *et al.*, *Econ. Geol.* 77, 1454 (1982).
6. T. N. Irvine *et al.*, *ibid.* **78**, 1287 (1983).
7. A. J. Naldrett and J. M. Duke, *Science* **208**, 1417 (1980); I. H. Campbell *et al.*, *J. Petrol.* **24**, 133 (1983); S.-J. Barnes *et al.*, *Chem. Geol.* **53**, 303 (1985); I. H. Campbell and S. J. Barnes, *Can. Min.* **22**, 151 (1985); S. J. Barnes and A. J. Naldrett, *J. Petrol.*, **27**, 791 (1986).
8. D. D. Lambert and E. C. Simmons, *Econ. Geol.* **83**, 1109 (1988).
9. T. N. Irvine and M. R. Sharpe, *Carnegie Inst. Washington Yearb.* **81**, 294 (1982); T. N. Irvine and M. R. Sharpe, in *Metallogeny of Basic and Ultrabasic Rocks*, M. J. Gallagher, R. A. Ixer, C. R. Neary, H. M. Prichard, Eds. (Institute of Mining and Metallurgy, London, 1986), pp. 183–198.
10. W. E. Cameron *et al.*, *Nature* **280**, 550 (1979).
11. R. H. Mitchell and R. R. Keays, *Geochim. Cosmochim. Acta* **45**, 2425 (1981); P. R. Hamlyn and R. R. Keays, *Econ. Geol.* **81**, 1431 (1986).
12. R. W. Kistler *et al.*, *J. Geophys. Res.* **74**, 3226 (1969); M. D. Fenton and G. Faure, *Geol. Soc. Am. Bull.* **80**, 1599 (1969).
13. D. J. DePaolo and G. J. Wasserburg, *Geochim. Cosmochim. Acta* **43**, 999 (1979).
14. G. A. McIntyre *et al.*, *J. Geophys. Res.* **71**, 5459 (1966); D. York, *Earth Planet. Sci. Lett.* **5**, 320 (1969).
15. G. K. Czamanske *et al.*, *Eos* **67**, 1251 (1986).
16. M. L. Zientek and E. M. Ripley, *U.S. Geol. Surv. Open-File Rep. 89–76* (1988).
17. D. D. Lambert, thesis, Colorado School of Mines (1982); ______ and E. C. Simmons, *Am. J. Sci.* **287**, 1 (1987).
18. Detailed mapping of the face of an ore-bearing horizon in the Stillwater platinum mine provided the opportunity to sample two of the four recognized varieties of the J-M Reef, Minneapolis Adit area, that are not well exposed at the surface [L. D. Raedeke and R. W. Vian, *Econ. Geol.* **81**, 1187 (1986)]. "Basal zone" ore straddles the base of OBZ I and allows sampling of U-type noritic or gabbroic cumulates stratigraphically beneath OBZ I in the LBS, as well as A-type olivine cumulates at the contact; "Main zone" ore typically occurs in troctolitic A-type cumulates stratigraphically higher in OBZ I. "Footwall zone" and "upper zone" ore were not observed in this face.
19. M. L. Zientek, thesis, Stanford University (1983); R. T. Helz, in *Stillwater Complex*, G. K. Czamanske and M. L. Zientek, Eds. (*Spec. Publ. 92*, Montana Bureau of Mines and Geology, Butte, 1985), pp. 97–117.
20. M. Lindner *et al.*, *Nature* **320**, 246 (1986).
21. G. Manhes *et al.*, *Earth Planet. Sci. Lett.* **47**, 370 (1980).
22. P. D. Nunes, *Geochim. Cosmochim. Acta* **45**, 1961 (1981); W. R. Premo *et al.*, *Geol. Soc. Am. Abst. Prog.* **18**, 722 (1986); H. A. Snyder *et al.*, *Eos* **68**, 429 (1987).
23. R. J. Walker and J. W. Morgan, *Science* **243**, 519 (1989).
24. R. J. Walker *et al.*, *Earth Planet. Sci. Lett.* **87**, 1 (1988).
25. N. J. Page *et al.*, in *Stillwater Complex*, G. K. Czamanske and M. L. Zientek, Eds. (*Spec. Publ. 92*, Montana Bureau of Mines and Geology, Butte, 1985), pp. 93–96.
26. A. J. Naldrett *et al.*, in *Origins of Igneous Layering*, I. Parsons, Ed. (NATO Advanced Science Institute Series, Reidel, Dordrecht, 1987), pp. 313–397; A. J. Naldrett and J. Lehmann, in *Geoplatinum 87*, H. M. Pritchard *et al.*, Eds. (Elsevier, London, 1988), pp. 93–110.
27. J. L. Wooden and P. A. Mueller, *Earth Planet. Sci. Lett.* **87**, 59 (1988); P. A. Mueller and J. L. Wooden, *Geology* **16**, 871 (1988).
28. I. S. McCallum, *Lunar Planet. Inst. Tech. Rep. 88–02*, 92 (1988).
29. R. J. Walker *et al.*, *Geochim. Cosmochim. Acta*, in press.
30. R. S. Cohen and R. K. O'Nions, *Earth Planet. Sci. Lett.* **61**, 73 (1982); W. M. White and P. J. Patchett, *ibid.* **67**, 167 (1984); J. D. Woodhead and D. G. Fraser, *Geochim. Cosmochim. Acta* **49**, 1925 (1985); C. Hawkesworth and R. Ellam, *Geology* **17**, 46 (1989).
31. J. W. Morgan *et al.*, *Tectonophysics* **75**, 47 (1981); J. W. Morgan, *J. Geophys. Res.* **91**, 12375 (1986).
32. J. W. Morgan and J. F. Lovering, *Earth Planet. Sci. Lett.* **3**, 219 (1967); J. Hertogen *et al.*, *Geochim. Cosmochim. Acta* **44**, 2125 (1980).
33. E. C. Simmons and G. N. Hanson, *Contrib. Mineral. Petrol.* **66**, 119 (1978); R. A. Wiebe, *Nature* **286**, 564 (1980).
34. Concentrations of Rb, Sr, Sm, and Nd and isotopic compositions of Sr and Nd were determined by conventional isotope dilution and thermal ioniza-

tion mass spectrometry [analytical procedures described in (*24, 29*)]. Osmium isotopic composition and Re and Os concentrations were determined with a sodium peroxide fusion technique and a resonance ionization mass spectrometer at the National Institute of Standards and Technology [R. J. Walker and J. D. Fassett, *Anal. Chem.* **58**, 2923 (1986); J. W. Morgan and R. J. Walker, *Anal. Chim. Acta*, in press].

35. S. R. Taylor and S. M. McLennan, *Philos. Trans. R. Soc. London Ser. A* **301**, 381 (1981).
36. S. B. Shirey and G. N. Hanson, *Geochim. Cosmochim. Acta* **50**, 2631 (1986).
37. We thank D. Vian for providing access to mine workings and samples of the J-M Reef and B. Lipin for providing samples of chromitites used in this study. The Mass Spectrometry group of the National Institute of Standards and Technology is thanked for the use of the RIMS instrument. Support of NASA grant NAGW-398 to G. Wetherill, NSF grant EAR8720836 to S. B. Shirey, R. W. Carlson, and L. Brown, and the Carnegie Institution of Washington is gratefully acknowledged. This manuscript was signficantly improved by the reviews of C. T. Barrie, M. Foose, B. Lipin, C. Martin, and an anonymous reviewer.

28 February 1989; accepted 24 April 1989

Potassium Channels in Cardiac Cells Activated by Arachidonic Acid and Phospholipids

DONGHEE KIM* AND DAVID E. CLAPHAM†

Two types of potassium-selective channels activated by intracellular arachidonic acid or phosphatidylcholine have been found in neonatal rat atrial cells. In inside-out patches, arachidonic acid and phosphatidylcholine each opened outwardly rectifying potassium-selective channels with conductances of 160 picosiemens ($I_{\text{K}\cdot\text{AA}}$) and 68 picosiemens ($I_{\text{K}\cdot\text{PC}}$), respectively. These potassium channels were not sensitive to internally applied adenosine triphosphate (ATP), magnesium, or calcium. Lowering the intracellular *p*H from 7.2 to 6.8 or 6.4 reversibly increased $I_{\text{K}\cdot\text{AA}}$ channel activity three- or tenfold, respectively. A number of fatty acid derivatives were tested for their ability to activate $I_{\text{K}\cdot\text{AA}}$. These potassium-selective channels may help explain the increase in potassium conductance observed in ischemic cells and raise the possibility that fatty acid derivatives act as second messengers.

MANY K^+ CHANNELS ARE MODULATED by intracellular second messengers. Most regulatory mechanisms described to date have involved soluble second messengers such as adenosine 3′,5′-monophosphate (cAMP). More recently, membrane-permeant lipophilic mediators, specifically arachidonic acid or its metabolites, have been shown to mediate signal transduction in neuronal and cardiac cells (*1, 2*). In cardiac cells, inwardly rectifying K^+ channels are controlled by intracellular Na^+ ($I_{\text{K}\cdot\text{Na}}$) (*3*), ATP ($I_{\text{K}\cdot\text{ATP}}$) (*4*), or guanine nucleotide binding protein (G) α and βγ subunits ($I_{\text{K}\cdot\text{ACh}}$) (*5*). The outwardly rectifying transient outward current (I_{TO}) (*6*) and the delayed rectifier current (I_{K}) are regulated by phosphorylation via protein kinase A or protein kinase C (*7*). We now report two outwardly rectifying K^+ channels in heart that open in response to certain fatty acid derivatives. We propose that lipid-soluble, intramembranous second messenger pathways may play an important role in channel gating.

Kim *et al.* showed that the βγ subunits of G proteins activate the inwardly rectifying, muscarinic-gated K^+ channel ($I_{\text{K}\cdot\text{ACh}}$) via stimulation of phospholipase A_2 (*2*). During our experiments with arachidonic acid, we noted the appearance of previously undescribed K^+ currents. These channels were distinct from atrial $I_{\text{K}\cdot\text{ACh}}$. Figure 1A shows whole-cell records of a rat neonatal atrial cell before and after intracellular perfusion with arachidonic acid. The current-voltage (*I-V*) relation immediately after breaking into the cell was similar to that measured in control cells (Fig. 1B) ($n = 8$). As the arachidonic acid diffused into the cells, both inward and outward currents developed within 2 to 4 min, increasing the slope conductance from 0.8 to 2.8 nS at 40 mV and from 0.9 to 1.7 nS at −120 mV. The increase in slope conductance was not due to nonspecific leakage. The inwardly rectifying current was completely blocked, and the outwardly rectifying current was partially blocked by 1 m*M* extracellular $BaCl_2$ (Fig. 1C). The outwardly rectifying current was not observed when intracellular CsCl replaced KCl, suggesting that arachidonic acid activated K^+-selective ionic currents. To determine the relative contributions from the many K^+ currents present, we studied currents at the single-channel level.

When an inside-out patch was formed in the presence of 10 μ*M* arachidonic acid in the bath, a high conductance channel ($I_{\text{K}\cdot\text{AA}}$) often appeared within 3 min. We rarely (<2%) observed this channel in control patches ($n > 100$) not exposed to arachidonic acid. Figure 2A shows the gradual increase in the opening frequency of the

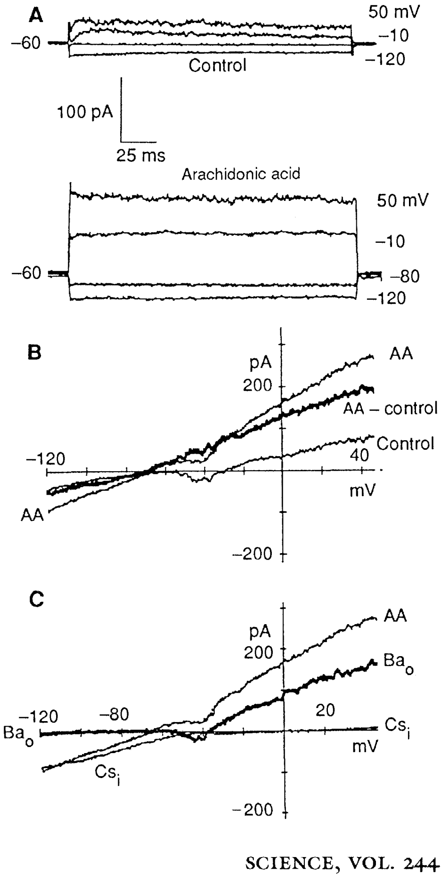

Fig. 1. Whole-cell currents produced by arachidonic acid. The pipette contained 140 m*M* K^+, 140 m*M* Cl^-, 5 m*M* EGTA, 2 m*M* Mg^{2+}, 10 m*M* Hepes (*p*H 7.2), and 10 μ*M* arachidonic acid. Extracellular solution contained 5 m*M* K^+, 140 m*M* Na^+, 1.0 m*M* Co^{2+}, 10 m*M* Hepes, 2 m*M* Mg^{2+}, and 3μ*M* tetrodotoxin (*p*H 7.2). (**A**) Control and arachidonic acid–induced currents in response to steps from a holding potential of −60 mV. (**B**) *I-V* relations. Immediately after the initiation of whole-cell recording, voltage ramps from −120 to 50 mV were made every 5 s from a holding potential of −60 mV. The *I-V* relations were taken 10 s (control) and 3 min (AA) after the initiation of whole-cell recording. The subtracted *I-V* relation (AA − control) is shown as the thick solid line. (**C**) $BaCl_2$ (1 m*M*) applied extracellularly, blocked the inwardly rectifying component of $I_{\text{K}\cdot\text{AA}}$. Intracellular recording with CsCl replacing KCl blocked the outward component of $I_{\text{K}\cdot\text{AA}}$ (separate recording). Rat heart cells were prepared by collagenase digestion of atria from 1- to 2-day-old newborn rat (*12*). Isolated single atrial cells were plated on glass cover slips and incubated in an atmosphere of 5% CO_2 and 95% air at 37°C until use 12 to 26 hours later. All experiments were performed at 22° ± 2°C. Currents were recorded with a LIST model EPC7 patch-clamp amplifier and recorded on a digital tape recorder. Records were filtered with an eight-pole Bessel filter at 2 kHz and analyzed with an INDEC 11/73 computer (*5*).

Department of Pharmacology, Mayo Foundation, Rochester, MN 55905.

*Present address: Department of Physiology, Chicago Medical School, North Chicago, IL 60064.

† To whom correspondence should be addressed.